Journal of Materials Chemistry A

Accepted Manuscript

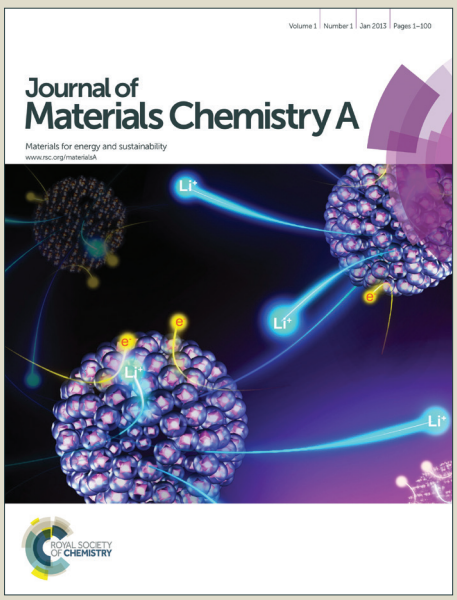

ROYAL SOCIETY OF CHEMISTRY

www.rsc.org/materialsA

Journal of
Materials Chemistry A

ARTICLE

Hydrothermal preparation of nanoporous TiO_2 films with exposed {001} facets and superior photocatalytic activity

Received 00th April 2015,
Accepted 00th January 20xx

DOI: 10.1039/x0xx00000x

www.rsc.org/

TongzhouXu,[ab] Hong Zheng,[*a] Pengyi Zhang,[*b] Wei Lin,[ab] Yumiko Sekiguchi[c]

TiO_2 films with exposed {001} facets and uniform nanopores in crystal facets were fabricated on the Ti-substrate with hydrothermal process followed by calcination at 600 °C. The effects of pretreatment of the Ti-substrate and the hydrothermal conditions (volume ratio of water/isopropanol, hydrothermal time, temperature and HF concentration) on the formation of nanopores in facetsof TiO_2 crystals were investigated. The sizes of nanopores can be controlled by adjusting the hydrothermal temperature. TG/DTA-MS analysis indicates that HF and isopropanol adsorbed on the Ti-substrate would be burned into gas and released during calcination. The effects of cleaning and heat treatment of the hydrothermally treated Ti-substrate indicate that residual organic matters and HF in TiO_2 facets and their transformation and reaction during calcination are essential for nanopores formation on the various facets of TiO_2 crystals. The as-prepared nanoporous TiO_2 films with exposed {001} facets exhibit much higher UV photocatalytic activity for the degradation of pharmaceuticals and personal care products than non-porous TiO_2 films with exposed {001} facets and P25 coated on the titanium sheet, revealing that the rational design and fabrication of the nanoporous TiO_2 films is an effective method to improve the photocatalytic activity.

1. Introduction

Titanium dioxide (TiO_2) has proved to be a versatile material among various oxide and non-oxide photocatalysts because of its high photocatalytic activity, low cost and long-term stability.[1-4] For anatase TiO_2, both theoretical and experimental studies have found that the minority {001} facets in the equilibrium state are more reactive than {101} facets.[5-8] While most anatase TiO_2 crystals are dominated with {101} facets, which are thermodynamically stable due to their lower average surface energy than that of {001} facets. Since the breakthrough in synthesizing anatase TiO_2 crystals with a large percentage of {001} facets in 2008,[8] many efforts have been focused on developing new routes for preparing TiO_2 with dominant {001} facets,[9-16] discussing their formation mechnisms,[17-19] and exploring their applications.[20,21] However, these photocatalysts are usually prepared in powder form, which has to be separated from the water in a slurry system after photocatalytic reaction and is inconvenient for many practical applications. This can be overcome by immobilizing TiO_2 particles as thin films on a solid substrate.[22] Moreover, direct growth of TiO_2 films with highly oriented anatase {001} facets on conductive substrates, that is, with free standing all-in-one structure, has also been realized.[23-26]

Nanoporous TiO_2 materials with large surface areas have proved to be excellent candidates for their many promising applications in environmental and energy areas.[27-29] In general, the properties and operational performance of nanoporous TiO_2 are largely dependent on its crystal phase, crystallinity, surface area, porosity, morphology and architecture. Zwilling et al.[30,31] gained amorphous TiO_2 porous film on metal titanium by anodic oxidation, with hydrofluoric acid (HF) as the electrolyte, which could be transformed into anatase TiO_2 after heat treatment. However, the thermal stability and the bonding strength between the porous film and the substrate need to be further improved. Herein, we demonstrated a simple strategy by combining appropriate pretreatment and subsequent hydrothermal process and calcination for fabricating the nanoporous TiO_2 films on the Ti-substrate, which has a large percentage of {001} facets and many nanopores in the crystal facets. The structure and morphologies of the nanoporous TiO_2 film could be rationally tailored by simply adjusting the synthetic parameters. And the studies of photocatalytic performance have clearly revealed that the as-prepared nanoporous TiO_2 films exhibited superior UV photocatalytic activities for the degradation of pharmaceuticals and personal care products (PPCPS), typical organic contaminants, than non-porous TiO_2 film with exposed{001} facets and P25 coated on the titanium sheet.

2. Experimental

2.1. Catalyst preparation

The fabrication strategy for the nanoporous TiO_2 film with exposed {001} facets is shown in **scheme 1**. In a typical preparation, metallic titanium (Ti) sheet (99.5% in purity) with a size of 100 mm × 240 mm × 0.12 mm was first etched in boiled 10% oxalic acid solution for 1.5 h to remove the oxide layer on the surface of Ti-sheet and used as both the starting material and the substrate of TiO_2 films. The pretreated Ti-sheet was immediately dipped in a 400 mL 0.03 M

[a.] Beijing Key Laboratory of Materials Utilization of Nonmetallic Minerals and Solid Wastes, National Laboratory of Mineral Materials, School of Materials Science and Technology, China University of Geosciences, Beijing 100083, China

[b.] State Key Joint Laboratory of Environment Simulation and Pollution Control, School of Environment, Tsinghua University, Beijing 100084, China

[c.] Corporate Research & Development Center, Toshiba Corporation, 1, Komukai-Toshiba-cho, Saiwaiku, Kawasaki 212-8582, Japan

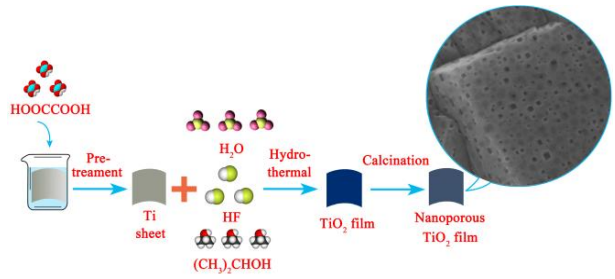

Scheme 1 Schematic illustration of the hydrothermal process combined with pretreatment of Ti-sheet in oxalic acid solution and calcination for the generation of nanoporous TiO_2 films with exposed {001} facets.

HF aqueous solution with isopropanol (the volume ratio of water/isopropanol was 2.2) in a Teflon-lined autoclave with total volume of 500 mL. After the hydrothermal treatment at 180 ℃ for 3h, the Ti-sheet was rinsed gently with deionized water and dried in air at room temperature, and finally calcined at 600 ℃ for 2 h. Then, the nanoporous TiO_2 film with exposed {001} facets was obtained. For comparison, the non-porous TiO_2 film also with exposed {001} facets was prepared in a similar method as reported by Sayed et al.[26] TiO_2 (Degussa P25) was coated on the titanium (Ti) sheet by dipping the pretreated Ti-sheet in P25 aqueous suspension (10 g/L) 15 times and then calcining at 400 ℃ for 90 min. As-prepared P25/Ti was used for reference in the photocatalytic activity test.

2.2. Characterization

The morphology of as-prepared nanoporous TiO_2 films with exposed {001} facets was observed with a field-emission scanning electron microscope (FESEM, S-5500, Hitachi) performed at an accelerating voltage of 5.0 kV. The high resolution transmission electron microscopy (HRTEM) analysis was conducted using a JEM-2011F electron microscopy (JEOL, Japan). To prepare the TEM specimen, the as-prepared nanoporous TiO_2 films on the Ti-sheet were first ultrasonically peeled in absolute ethanol for 40 min and then the suspension was dropped on a carbon film supported on copper grid and dried in air before analysis. The adsorption of krypton at 77.4 K was performed on a Micromeritics TriStar II 3020 adsorption apparatus. The Brunauer-Emmett-Teller (BET) specific surface area was determined by a multi-point method using adsorption data in the relative pressure (P/P0) range of 0.05-0.3. In addition to the direct measurement of TiO_2 films on the Ti-sheet, powder species scratched from the Ti-sheet were also measured. The X-ray diffraction (XRD) measurements were carried out on a Rigaku D/max-RB with Cu Kα radiation (λ= 0.15418 nm), operated at 40 kV and 100 mA. Chemical states of surface elements were investigated by X-ray photoelectron spectroscopy (XPS, PHI-5300, ESCA) at a pass energy of 50 eV, using Al Kα as an exciting X-ray source. All the binding energies were referenced to the C_{1s} peak at 284.8 eV. Photo-electrochemical measurements were performed in a three-electrode quartz cell containing 0.1 M Na_2SO_4 electrolyte solution. Platinum wire was used as the counter electrode, and saturated calomel electrode (SCE) was used as the reference electrode. The as-prepared nanoporous TiO_2 films with a size of 20 mm × 40 mm served as the working electrode. The UV irradiation was provided by a 10 W low-pressure mercury lamp (λ_{max} = 254 nm). The photo-electrochemical experiment results were recorded by using an electrochemical system (CHI-660C, China). The photo-currents of the photocatalysts to UV light were measured at 0 V with reference to SCE. The powders remained on the internal wall of the autoclave after hydrothermal reaction were analyzed by a simultaneous TG/DTA-MS apparatus containing an STD 2960 simultaneous TG/DTA (TA Instruments Inc.) thermal analyzer and a Thermostar GSD 300 (Balzers Instruments) quadrupole mass spectrometer. Coupling between the two parts was provided through a heated 100% methyl deactivated fused silica capillary tube kept at 200 ℃. A mass range between *m*/*z*=1~100 was monitored through 64 channels in multiple ion detection mode (MID). Measuring time was ca. 0.5 s for a channel. About 50 mg of the powder was heated in the mixed atmosphere with N_2/O_2 (1:1,volume ratio) at a heating rate of 5 ℃ min^{-1} from 0 to 800 ℃. Pure-$Al_2O_3$was used as the reference material.

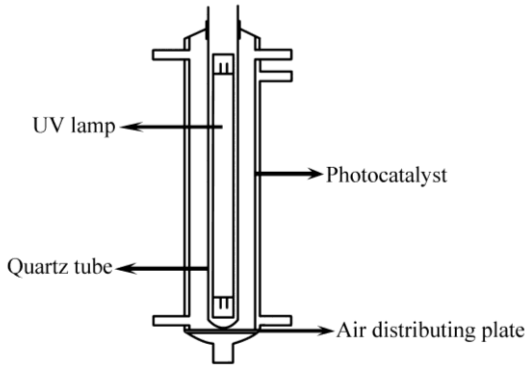

Fig. 1 Experimental setup for evaluating the photocatalytic activity.

2.3. Photocatalytic activity test

The photocatalytic activity of as-prepared TiO_2 films was measured by taking 2 mg L^{-1} of ethenzamide aqueous solution in a 150mL cylindrical vessel (**Fig. 1**) into which a 100 mm ×120 mm of as-prepare TiO_2 film was inserted and attached to the inner wall. A 10 W low-pressure mercury lamp (λ_{max} = 254 nm) served as the light source. Oxygen gas was bubbled from the bottom of the reactor at the flow rate of 30 mL min^{-1}. After the adsorption reached equilibrium in dark for 30 min, the UV lamp was turned on to start the photocatalytic degradation reaction. Aliquots were taken out every 5min and the concentration of ethenzamide was analyzed by a high performance liquid chromatography (LC-10AD, Shimadzu, Japan) with a UV detector (SPD-10AV) at 230 nm and a Kromasil C18 column (250 mm × 4.6 mm) for separation. The mobile phase was a mixture of methanol and water (2:1 v/v) at a flow rate of 1.5 mL min^{-1}.

To check the stability of as-prepared nanoporous TiO_2 films with exposed {001} facets, the UV photocatalytic activity of the catalyst to degrade ethenzamide was continuously tested for 5 times and each test lasted 45 min. Before each test, the nanoporous TiO_2 film was rinsed with deionized water and irradiated for 10 min in ultrapure water by UV light.

3. Results and discussion

3.1. Characterization of as-prepared samples

Fig. 2A shows the typical scanning electron microscopy (SEM) images of the nanoporous TiO_2 film with exposed {001} facets. The exposed surface of the film consists of truncated tetrahedrons with well patterned major flat and square top surfaces and minor four isosceles trapezoidal lateral surfaces. Based on the geometrical symmetry of anatase TiO_2, the top and lateral surfaces are {001} and {101} facets, respectively.[8] It can be clearly seen from the enlarged SEM image (as shown in the inset of **Fig. 2A**) that the average size of {001} facets is ca. 830 nm and many uniform nanopores occurred in both {001} facets and {101} facets. The amount and shape of

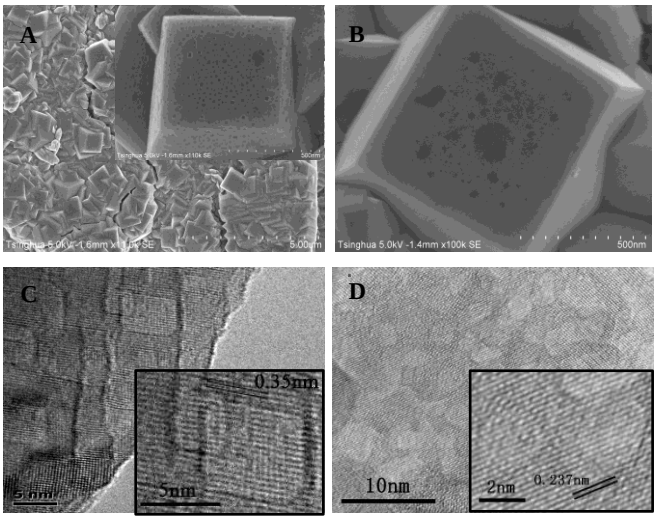

Fig. 2 (A) FE-SEM images of typical nanoporous TiO_2 film with exposed {001} facets (inset: the enlarged nanoporous TiO_2); (B) FE-SEM images of non-porous TiO_2 film with exposed {001} facets; (C and D) HR-TEM images of the nanoporous TiO_2 sample scratched off from the Ti-substrate.

pores for nanoporous TiO_2 and non-porous TiO_2 films were compared with Image-Pro Plus software after the SEM images were modified into black and white images by changing the contrast and brightness with PhotoImpact. Over 700 nanopores were found to occur on every {001} facet of nanoporous TiO_2 film, while only some asymmetric shallow pits on {001} facets were observed for non-porous TiO_2 film (**Fig. 2B**). The exposed {001} facets and porous structure were also confirmed by HR-TEM image of TiO_2 samples scratched from the Ti-substrate (**Fig. 2C** and **D**). Some overlapping rectangular pores with rounded corners and the size of (~2-25) nm × (~2-15) nm were clearly observed in the facets of TiO_2. The lattice spacing of 0.35 nm corresponds to the (101) planes, while the lattice spacing of 0.237nm corresponds to the (004) planes, further confirming the presence of {001} facetsin the nanoporous TiO_2 films.[13] In addition, the continuous stripe and same lattice spacing indicate that the bottom surface of nanopores has the same facet as that in which nanopores located. The BET specific surface areas by krypton adsorption of the nanoporous TiO_2 powder scratched from Ti-sheet was 6.12 m^2 g^{-1}, while that of the non-porous TiO_2 was 5.15 m^2 g^{-1}. Krypton adsorption at liquid nitrogen temperature (i.e. 77.4 K) can improve the detection limit significantly and allows to determine absolute surface areas down to 0.05 m^2 or less, and is recommended to low surface area analysis. And the ratio of surface area to apparent area of the nanoporous TiO_2 film was 72.0 m^2 m^{-2} Ti-sheet, which is much higher than that of the non-porous TiO_2 film (59.5 m^2/m^2 Ti-sheet).

Fig. 3A shows the X-ray diffraction (XRD) patterns of the as-prepared TiO_2 films. It can be clearly seen that anatase is the main crystal phase and rutile coexisted in both nanoporous and non-porous TiO_2 films with exposed {001} facets. The ratio of rutile (W_R) and anatase (W_A) in both TiO_2 films were calculated as follows.[32]

$$W_R = 1/(1 + 0.8 * I_A/I_R) \quad (1)$$

$$W_A = 1 - W_R \quad (2)$$

where I_A and I_R represent the diffraction intensities of anatase (101) and rutile (110), respectively. Almost identical rutile content was found in the nanoporous (31%) and non-porous (30%) TiO_2 films. The percentage of {001} facet was calculated by the intensity of diffraction peak of (004) facet and (101) facet of anatase TiO_2, and

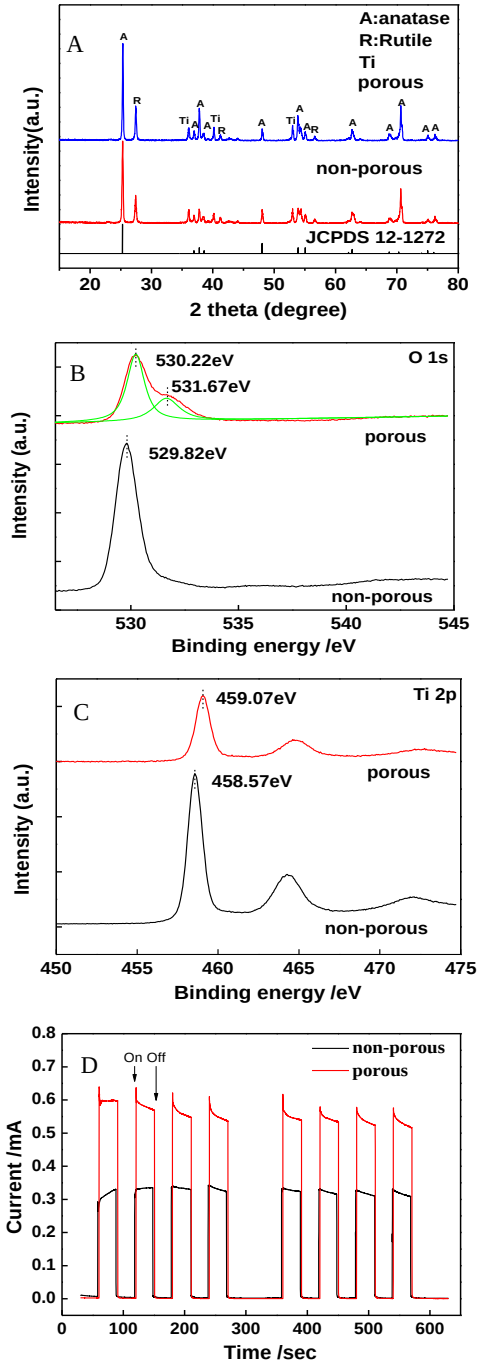

Fig. 3 (A) XRD patterns; high resolution XPS spectra: (B) O 1s and (C) Ti 2p; and (D) photocurrent-time testing curves of as-prepared TiO_2 films.

was found to be 58%, which is close to 57% of non-porous TiO_2 film reported by Sayed et al.[26]

From XPS spectra of the nanoporous TiO_2 films as shown in **Fig. 3B** and **C**, we can see that the peaks of O 1s spectrum can be divided into two peaks centered at 530.22 and 531.67 eV, which can be assigned to lattice oxygen of the Ti-O bond and surface hydroxyl groups,[33] respectively. The surface hydroxyl groups likely correspond to Ti-OH on the TiO_2 surface and in the nanopores.[34] These surface hydroxyl groups, acting as an electron donor for photo-generated h^+, can be oxidized into hydroxyl radicals (·OH)[35], accordingly improving the separation of photogenerated carriers and photocatalytic activity. In addition, compared with the non-porous

TiO_2 film, the peaks of Ti 2p and O 1s of the nanoporous TiO_2 film shifted towards higher binding energy values (from 458.57 to 459.07 eV and from 529.82 to 530.22 eV, respectively), which indicates that less electron density remains on the Ti and O of the nanoporous TiO_2 film than the non-porous TiO_2 film. It is hypothesized that oxygen atoms adjacent to oxygen defect sites caused by nanopores donate some of their electron density toward titanium atoms that are not fully coordinated. This donation of electron density toward the Titanium makes the O 1s peak shift toward the higher binding energy.[36,37] The existence of these oxygen vacancy and surface hydroxyl groups can also exert the effects on photocurrent of the nanoporous TiO_2 film. As shown in **Fig. 3D**, the photocurrent of the nanoporous TiO_2 film under UV light is much larger than that of the non-porous TiO_2 film with similar dimension, thickness and active facets, confirming that the existence of nanopores is conducive to separation of photogenerated carriers.[38,39] Thus, it can be expected that the nanoporous TiO_2 films may have high photocatalytic activity for degrading pollutants.[39]

3.2. Nanopores formation mechanism

To learn more about the mechanism of many nanopores formed in the facets of TiO_2 crystals, the morphology of the TiO_2 films prepared in different conditions were investigated. As shown in **Fig. 4A**, if the Ti-sheet was not pretreated in oxalic acid solution, the formed TiO_2 films easily fell off from the substrate and the {001} facets of truncated bipyramids were largely eroded (**Fig. 4B**). In addition, if the pretreated Ti-sheet was kept in air for a period of time before the hydrothermal process, we can't obtain the nanoporous TiO_2 films either (not shown). Thus, we think the removal of the inert oxide layer on the surface of Ti substrate by boiled oxalic acid makes the fresh metallic Ti exposed and promotes the formation and stability of the nanoporous TiO_2 films on the substrate. Furthermore, we found the volume ratio of water/isopropanol also affected the formation of nanopores. Isopropanol acts not only as reaction medium but also as protecting agent to control the isotropic growth of anatase TiO_2 crystals.[11] The addition of isopropanol is proved to influence the growth of {001} facets of TiO_2 greatly.[11,26] Isopropanol may dissociate to form an alkoxy group ($(CH_3)_2CHO$-) bound to coordinative unsaturated Ti^{4+} cations on the (001) and (101) surfaces.[11] The higher density of 5-fold Ti atoms on (001) surfaces may lead to more obvious selective adhesion of isopropanol, which retards the growth of anatase TiO_2 single crystals along {001} direction. When the volume ratio of water/isopropanol increased from 2.2 to 4.4, although (001) facet of TiO_2 crystal can be formed, only a few nanopores were observed (**Fig. 4C**). When the volume ratio of water/isopropanol was decreased to 1.1, similar results occurred (**Fig. 4D**).

In addition, the effects of hydrothermal time, hydrothermal temperature and HF concentration were investigated. As shown in **Fig. 4E**, after 2 h of hydrothermal reaction the truncated tetrahedrons with several tiny pores were observed, but the rounded corners were found on {001} facets and{101} facets, indicating that TiO_2 crystal was not completely formed. However, if the hydrothermal time was prolonged to 5 h, only a few nanopores and pits formed (**Fig. 4F**), indicating the importance of the appropriate hydrothermal time for forming nanoporous TiO_2 films. **Fig. 4G** shows that when the hydrothermal temperature was 170 ℃ uniform nanopores were also formed, which is similar to those observed when the hydrothermal temperature was 180 ℃. While much smaller nanopores were uniformly formed when the hydrothermal temperature was increased to 190 ℃ (**Fig. 4H**). Therefore, the sizes of nanopores in the facets can be simply controlled by adjusting the hydrothermal temperature. It is well known that HF can act as a capping agent.[40] Besides, it also has strong corrosion ability. In the acidic HF solution, Ti-OH would be replaced by Ti-F through ligand exchange between surface hydroxyl groups and fluoride ions.[4,8] **Fig. 4I** shows when the HF concentration was 0.025 M, {001} facets were formed but few nanopores were found, indicating no enough HF can be used to further erode the TiO_2 facets. When the HF concentration was increased to 0.04M, there were still many uniform nanopores on TiO_2 facets, the size of pores became larger and the boundary of TiO_2 facets was slightly corroded (**Fig. 4J**).

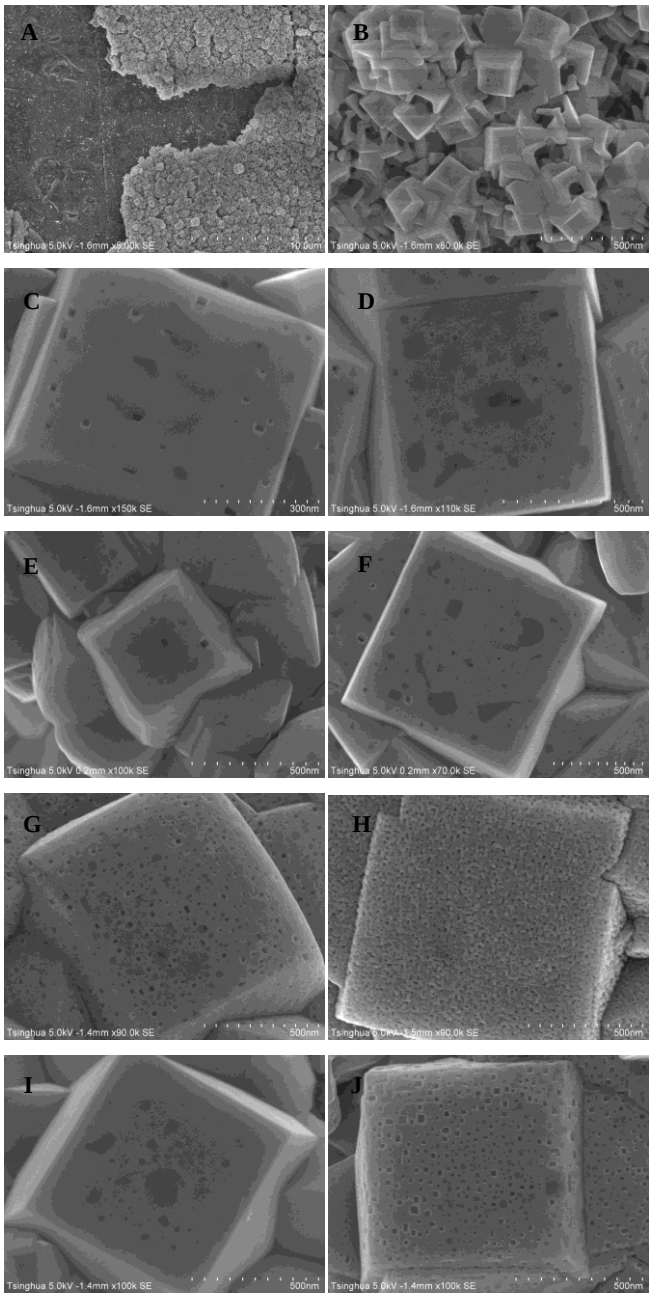

Fig. 4 (A and B) FE-SEM images of Ti-sheet after the hydrothermal treatment without pretreatment of Ti-sheet in oxalic acid solution; (C and D) FE-SEM images of Ti-sheet after the hydrothermal treatment with the volume ratio of water/isopropanol of 4.4 (C) and1.1 (D); (E and F) FE-SEM images of Ti-sheet after the hydrothermal treatment for 2 h (E) and 5 h (F); (G and H) FE-SEM images of Ti-sheet after the hydrothermal treatment at 170 ℃ (G) and 190 ℃ (H); (I and J) FE-SEM images of Ti-sheet after the hydrothermal treatments by using 0.025 M (I) and 0.04 M (J) of HF concentrations.

In order to further clarify the formation mechanism of the nanoporous TiO_2 films, the powders remained on the internal wall of autoclave after hydrothermal reaction were collected and analyzed by thermogravimetry (TG). From the results of the TG and differential thermal analysis (DTA) shown in **Fig. 5A**, we can see that two obvious endothermic peaks appeared at 200-350 ℃ and 400-600 ℃, respectively. Simultaneous detection by mass spectrum (**Fig. 5B**) revealed that the first mass loss (200-350 ℃) was caused mostly by release of H_2O and a small part by CO_2 from burning of some residual organic matters, and the second mass loss (400-600 ℃) was caused mostly by the endothermic CO_2 formation and a small part by release of HF adsorbed on TiO_2 surface. These results indicate that HF adsorbed on Ti-substrate and CO_2 burned from adsorbed isopropanol would be released as gas during the calcination at 600 ℃. Thus we think the release of these gaseous compounds in combination with strong corrosion capability of HF during calcination at temperature as high as 600 ℃ are vital to the formation of nanopores in the facets of TiO_2 crystals.

To verify the above assumption, we investigated the effects of cleaning and heat treatment on the pore formation in TiO_2 facets. After treated in the hydrothermal process, the Ti-sheet was ultrasonically cleaned in water or in ethanol, followed by heat treatment at 100 ℃ or 600 ℃ for 2 h. SEM images of the Ti-sheets after treated at different conditions are shown in **Fig.6**. We can see the obvious effects of ultrasonic cleaning on the pore formation. When the Ti-sheet was ultrasonically cleaned in deionized water followed by heat treatment at 100 ℃, no nanopores were found in any facets except for some residual organic matters (**Fig. 6A**). In addition, when the Ti-sheet was calcined at 600 ℃ not at 100 ℃, many very small and shallow pores appeared in TiO_2 facets (**Fig. 6B**). If the obtained Ti-sheet was ultrasonically cleaned in ethanol before calcination, no obvious nanopores appeared whatever it was further calcined at 100 ℃or 600 ℃ (**Fig. 6C** and **D**). However, if the Ti-sheet was not ultrasonically cleaned in water or in ethanol but directly calcined at 600 ℃, many uniform nanopores appeared in TiO_2 facets (**Fig. 6 F**). But if it was only treated at 100 ℃ not at 600 ℃, no nanopores formed in any facets either (**Fig.6E**). These results indicate that if the hydrothermally processed Ti-sheet is cleaned enough, i.e. adsorbed isopropanol and HF are washed out from the Ti-substrate; or if it is not calcined at high temperature, no nanopores will be formed in TiO_2 facets. Thus, we can conclude that residual organic matters and HF in TiO_2 facets and their transformation and reaction during calcinations are essential for nanopores formation in the various facets of TiO_2. During calcination, residual organic matters are burned off and simultaneously TiO_2 crystal surface is corroded by HF, accordingly many nanopores are generated in TiO_2facets.

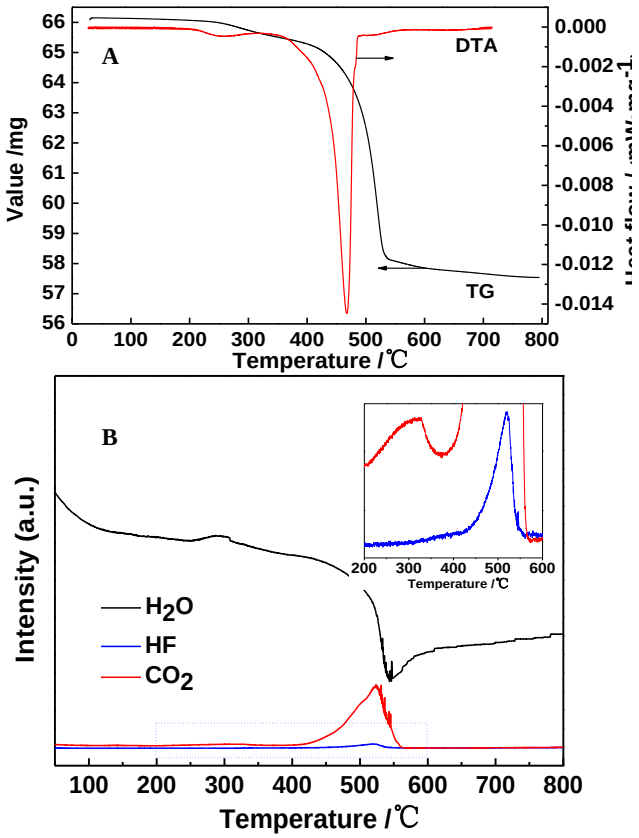

Fig. 5 (A) TG and DTA diagram; (B) simultaneous detection by mass spectroscope (inset: magnified mass spectroscope of CO_2 and HF) of TiO_2 powders collected from the internal wall of the autoclave after hydrothermal reaction.

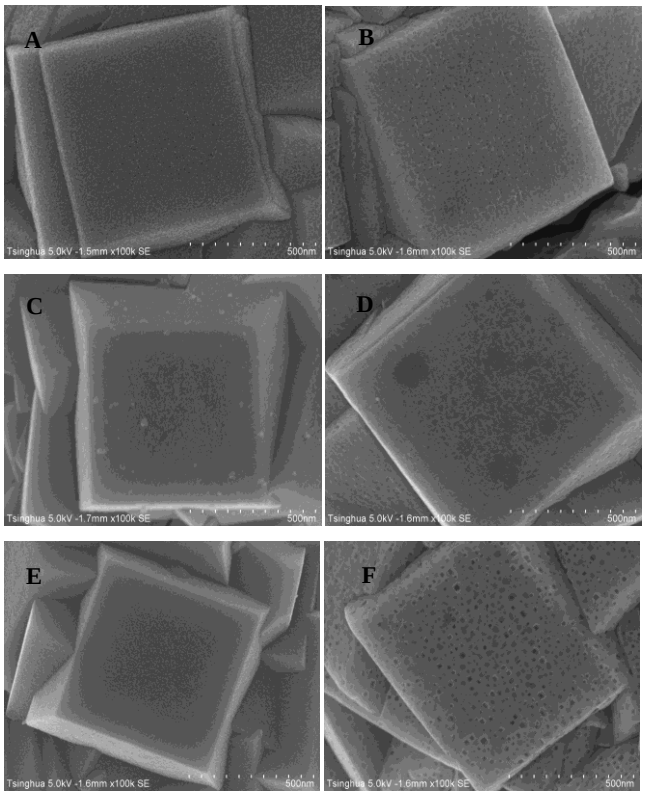

Fig. 6 SEM images of Ti-plates after treated at different conditions (A) heated at 100 ℃ for 2 h after ultrasonicated in deionized water; (B) calcined at 600 ℃ for 2 h after ultrasonicated in deionized water; (C) heated at 100 ℃ for 2 h after ultrasonicated in ethanol; (D) calcined at 600 ℃ for 2 h after ultrasonicated in ethanol; (E) heated at 100 ℃ for 2 h after rinsed gently with pure water; (F) calcined at 600 ℃ for 2 h after rinsed gently with pure water.

3.3. Photocatalytic activity of as-prepared samples

The photocatalytic activity of as-prepared nanoporous TiO_2 films was evaluated for the degradation of ethenzamide under 254 nm UV illumination. Ethenzamide is one of the typical pharmaceuticals and personal care products (PPCPs), which has high solubility in water and has been widely detected in the environment.[41,42] As shown in **Fig. 7**, the nanoporous TiO_2 films exhibited much higher activity than those of non-porous TiO_2 with similar dimension, thickness and active facets and P25 coated on the Ti-sheet under identical

experimental conditions. The photocatalytic decomposition of ethenzamide by different catalysts was in accordance with the first-order kinetics. The corresponding rate constant over the nanoporousTiO_2 films was 0.091 min^{-1}, which is nearly increased 56.9% compared with that of the non-porous TiO_2 films (0.058 min^{-1}) and almost 2.3 times higher than P25 coated on the Ti-sheet (0.028 min^{-1}). Superior photocatalytic activity of the nanoporous TiO_2 film is consistent with the results of BET, XPS and photo-current analyses. The reason that the nanoporous TiO_2 film possesses higher

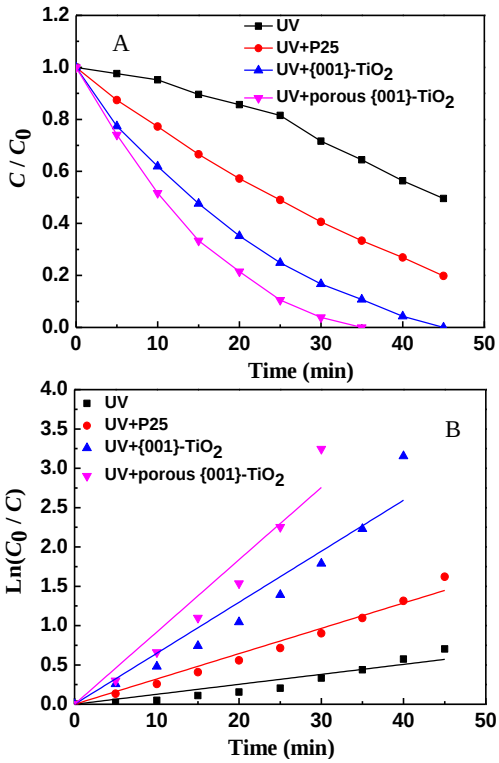

Fig. 7 (A) UV photocatalytic activity of nanoporous TiO_2 films with exposed {001} facets for the degradation of ethenzamide; (B) plots of ln(C_0/C) *versus* illumination time representing the fitting using the pseudo-first-order reaction of nanoporous TiO_2 films with exposed {001} facets.

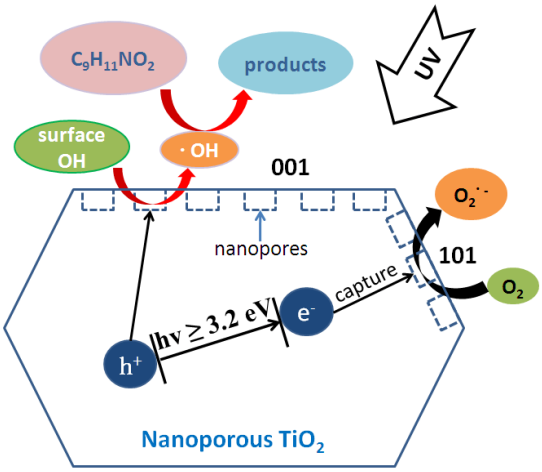

Fig. 8 Mechanism of electron-hole separation in TiO_2 with exposed {001} and {101} facets under UV irradiation, which is improved by nanopores in the TiO_2facets.

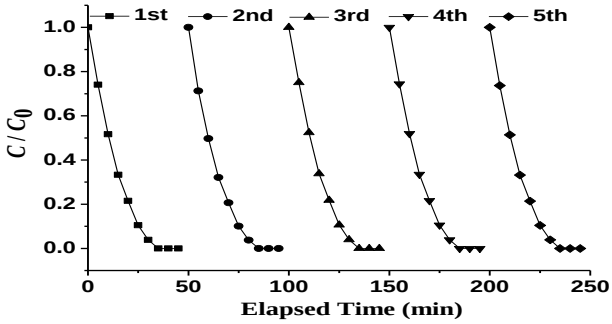

Fig. 9 Cycling runs of nanoporous TiO_2 films with exposed {001} facets for the degradation of ethenzamide under UV irradiation.

activity than non-porous TiO_2 film is shown in **Fig. 8**. First, as illustrated by TEM, the bottom surface of nanopores in {001} facets also showed the {001} facets, while those in {101} facets had the {101} facets. Because photogenerated electrons tend to transport to {101} facet with higher positive surface potential and photogenerated holes tend to transport to {001} facet with lower positive surface potential,[43] nanopores provide more surface area to improve the separation of photogenerated carriers. In addition, surface hydroxyl groups caused by nanopores are beneficial to transform holes into hydroxyl radicals. Thus, the formation of nanopores in TiO_2 facets not only provides larger surface area for reaction, but also enhance the charge separation and generation of hydroxyl radicals, as a result the photocatalytic activity is significantly increased.

To further evaluate its stability and reusability, the nanoporous TiO_2 film with exposed {001} facets was repeatedly used for five cycles, and its photocatalytic performances are shown in **Fig. 9**. It can be found that the as-prepared nanoporous TiO_2 films maintained a stable and high photocatalytic activity for the degradation of ethenzamide during all the five cycles. These results indicate that the nanoporous TiO_2 films with exposed {001} facets can serve as a stable and efficient UV photocatalyst.

4. Conclusions

In summary, the nanoporous TiO_2 films with exposed {001} facets and many pores uniformly distributed in crystal facets have been successfully fabricated on the Ti-substrate by a hydrothermal process in combination of subsequent calcination. The pretreatment of the Ti-substrate in boiled oxalic acid, the presence of isopropanol and HF adsorbed in the hydrothermally treated Ti-sheet and their transformation and reaction during calcination at high temperature are vital to the formation of nanopores in facets of TiO_2 crystals. As-prepared nanoporous TiO_2 films with exposed {001} facets exhibit much higher photocatalytic activity than the non-porous TiO_2 films and P25 coated on the Ti-sheet for the degradation of a typical pharmaceutical pollutant generally found in the water environment.

Acknowledgements

This work was funded by the National Basic Research Program of China (2013CB632403), Science Fund for Creative Research Groups (21221004), Tsinghua - Toshiba Energy and Environment Research Center, the Collaborative Innovation Center for Regional Environmental Quality, and the Fundamental Research Funds for the Central Universities (2652015311, 2652015261, 2652014113).

References

1 M. Liu, L. Piao, W. Lu, S. Ju, L. Zhao, C. Zhou, H. Li and W. Wang, *Nanoscale*, 2010, **2**, 1115.
2 G. Wu, J. Wang, D. F. Thomas and A. Chen, *Langmuir*, 2008, **24**, 3503.
3 J. Yu, L. Qi and M. Jaroniec, *J. Phys. Chem. C*, 2010, **114**, 13118.
4 S. Liu, J. Yu and M. Jaroniec, *J. Am. Chem. Soc.*, 2010, **132**, 11914.
5 X. Q. Gong and A. Selloni, *J. Phys. Chem. B*, 2005, **109**, 19560.
6 M. Lazzeri, A. Vittadini and A. Selloni, *Phys. Rev. B*, 2002, **65**, 119901.
7 M. Lazzeri, A. Vittadini and A. Selloni, *Phys. Rev. B*, 2001, **63**, 155409.
8 H. G. Yang, C. H. Sun, S. Z. Qiao, J. Zou, G. Liu, S. C. Smith, H. M. Cheng and G. Q. Lu, *Nature*, 2008, **453**, 638.
9 X. Han, Q. Kuang, M. Jin, Z. Xie and L. Zheng, *J. Am. Chem. Soc.*, 2009, **131**, 3152.
10 Y. Alivov and Z. Y. Fan, *J. Phys. Chem. C*, 2009, **113**, 12954.
11 H. G. Yang, G. Liu, S. Z. Qiao, C. H. Sun, Y. G. Jim, S. C. Smith, J. Zou, H. M. Cheng and G. Q. Lu, *J. Am. Chem. Soc.*, 2009, **131**, 4078.
12 X. Han, X. Wang, S. Xie, Q. Kuang, J. Ouyang, Z. Xie and L. Zheng, *Rsc Adv.*, 2012, **2**, 3251.
13 L. Wu, B. X. Yang, X. H. Yang, Z. G. Chen, Z. Li, H. J. Zhao, X. Q. Gong and H. G. Yang, *CrystEngComm*, 2013, **15**, 3252.
14 D. Zhang, G. Li, X. Yang and J. C. Yu, *Chem. Commun.*, 2009, 4381.
15 Y. Dai, C. M. Cobley, J. Zeng, Y. Sun and Y. Xia, *Nano. Lett.*, 2009, **9**, 2455.
16 Z. Lai, F. Peng, Y. Wang, H. Wang, H. Yu, P. Liu and H. Zhao, *J. Mater. Chem.*, 2012, **22**, 23906.
17 P. Liu, Y. Wang, H. Zhang, T. An, H. Yang, Z. Tang, W. Cai and H. Zhao, *Small*, 2012, **8**, 3664.
18 Y. Wang, H. Zhang, Y. Han, P. Liu, X. Yao and H. Zhao, *Chem. Commun.*, 2011, **47**, 2829.
19 H. Zhang, X. Liu, Y. Li, Y. Li and H. Zhao, *Sci. China Chem.*, 2013, **56**, 402.
20 Y. Yu, X. Wang, H. Sun and M. Ahmad, *Rsc Adv.*, 2012, **2**, 7901.
21 J. Yu, J. Fan and K. Lv, *Nanoscale*, 2010, **2**, 2144.
22 J. G. Yu, H. G. Yu, B. Cheng, X. J. Zhao, J. C. Yu and W. K. Ho, *J. Phys. Chem. B*, 2003, **107**, 13871.
23 Q. Xiang, J. Yu and M. Jaroniec, *Chem. Commun.*, 2011, **47**, 4532.
24 X. Wang, G. Liu, L. Wang, J. Pan, G. Q. Lu and H. M. Cheng, *J. Mater. Chem.*, 2011, **21**, 869.
25 H. Zhang, Y. Wang, P. Liu, Y. Han, X. Yao, J. Zou, H. Cheng and H. Zhao, *ACS Appl. Mater. Inter.*, 2011, **3**, 2472.
26 M. Sayed, P. Fu, H. M. Khan and P. Zhang, *Int. J. Photoenergy*, 2014, **2014**, 490264.
27 Y. Ren, L. J. Hardwick and P. G. Bruce, *Angew. Chem. Int. Ed., 2010, 49, 2570.*
28 D. Kim, K. Lee, P. Roy, B. I. Birajdar, E. Spiecker and P. Schmuki, *Angew. Chem. Int. Ed.*, 2009, **48**, 9326.
29 J. Wang, Z. Bian, J. Zhu and H. Li, *J. Mater. Chem. A*, 2013, **1**, 1296.
30 V. Zwilling, E. Darque-Ceretti, A. Boutry-Forveille, D. David, M. Y. Perrin and M. Aucouturier, *Surf. Interface Anal.*, 1999, **27**, 629.
31 V. Zwilling, M. Aucouturier and E. Darque-Ceretti, *Electrochim. Acta*, 1999, **45**, 921.
32 G. Liu, Z. Chen, C. Dong, Y. Zhao, F. Li, G. Q. Lu and H. M. Cheng, *J. Phys. Chem. B*, 2006, **110**, 20823.
33 P. Fu, Y. Luan and X. Dai, *J. Mol. Catal. A: Chem.*, 2004, **221**, 81.
34 M. R. Hoffmann, S. T. Martin, W. Choi and D. W. Bahnemann, *Chem. Rev.*, 1995, **95**, 69.
35 A. Fujishima, T. N. Rao and D. A. Tryk, *J. Photochem. Photobio. C: Photochem. Rev.*, 2000, **1**, 1.
36 C. Donley, D. Dunphy, D. Paine, C. Carter, K. Nebesny, P. Lee, D. Alloway and N. R. Armstrong, *Langmuir*, 2002, **18**, 450.
37 Z. Li, P. Zhang, T. Shao, J. Wang, L. Jin and X. Li, *J. Hazard. Mater.*, 2013, **260**, 40.
38 N. Chandrasekharan and P. V. Kamat, *J. Phys. Chem. B*, 2000, **104**, 10851.
39 Z. Bian, T. Tachikawa and T. Majima, *J. Phys. Chem. Lett.*, 2012, **3**, 1422.
40 J. M. Wu and M. L. Tang, *J. Hazard. Mater.*, 2011, **190**, 566.
41 K. Kuroda, M. Murakami, K. Oguma, Y. Muramatsu, H. Takada and S. Takizawa, *Environ. Sci. Technol.*, 2012, **46**, 1455.
42 N. Nakada, K. Kiri, H. Shinohara, A. Harada, K. Kuroda, S. Takizawa and H. Takada, *Environ. Sci. Technol.*, 2008, **42**, 6347.
43 R. Hengerer, L. Kavan, P. Krtil, M. Gratzel, *J. Electrochem. Soc.*, 2000, **147**, 1467.

A table of contents entry

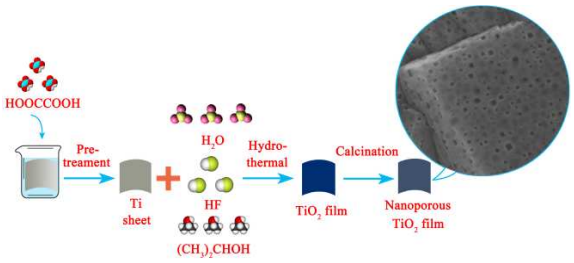

Nanoporous TiO_2 film with numerous pores in {001} facets shows high photocatalytic activity for pharmaceutical pollutants